COMPARISON OF TWO DRY VIBRATABLE TUNDISH LININGS THROUGH LABORATORY EXPERIMENTS

Tyler Richards*, Jeffrey Smith, Ronald O'Malley, Todd Sander
Missouri University of Science and Technology, Rolla, MO, USA

ABSTRACT

A rotating disc experiment was employed to replicate the interactions between molten steel and dry vibratable material (DVM) used for tundish linings. Two compositions of DVM were tested, both of which are commercially available: one containing approximately 70 wt% periclase (MgO) and 30 wt% olivine ((Mg,Fe)2SiO4), the other containing periclase with no olivine. The exposed refractory samples were analyzed using cathodoluminescence, backscattered scanning electron microscopy, energy dispersive spectroscopy, and X-ray diffraction. These results are compared to post-mortem samples obtained from industry supplied tundish lining samples. These investigations provide insight into the mechanics of refractory corrosion in the continuous casting of steel, as well as how these interactions influence the quality of the final steel product.

INTRODUCTION

In continuous casting, a tundish is used as an intermediate vessel that allows for multiple ladles of steel to be cast consecutively without interruption to the flow of steel into the mold. In addition, residence in the tundish provides time to float out inclusions and improve thermal and chemical homogeneity.

Tundishes utilize a disposable refractory lining that is typically changed between casting sequences. Tundish linings have been applied in various ways. In the past, bricks or boards were used. Today its more common to install linings as a sprayable mixture or dry vibratable material (DVM). DVM tundish linings are installed by pouring material between the tundish form (typically a steel shell lined with a permanent alumina-based backup lining) and a removeable mandrel. The mandrel can vibrate to aid in packing in material, as well as apply heat to cure the lining, which contains a phenolic resin binder. This technology is of interest to steelmakers as the lack of water mitigates any need to dry out the lining first, and the use of a mandrel ensure consistent and smooth surfaces when compared to sprayed linings.

Many linings in use today primarily contain magnesia, often in the form of periclase. The periclase used in these linings consist of MgO aggregates with crystallites on the order of 10-100 μm bound with a calcium magnesium silicate phase like monticellite ($CaMgSiO_4$)[1]. In addition, some linings contain other oxides like chromite ($(Mg,Fe)Cr_2O_4$) or Mg-rich olivine ($(Mg,Fe)_2SiO_4$)[2]. These oxides were added with the intent of improving corrosion resistance to the fluxes added to the surface of the liquid steel[2,3].

High-MgO tundish linings may be a concern for steelmakers who use Al to deoxidize their steel. This is due to the possible generation of magnesium aluminate spinel inclusions. There are multiple theories into how spinel forms. These often involve either the direct reaction of MgO and Al_2O_3 to form $MgAl_2O_4$[4] or reduction of MgO into Mg vapor, which subsequently reacts with an alumina inclusion in the steel[5].

The goal of this paper is to compare two DVM tundish linings, one consisting of

periclase and olivine, the other containing periclase but no olivine. Comparisons are made by way of post-mortem analysis of industrial samples as well as a rotating dip test conducted in the lab.

PROCEDURE

Post-Mortem

Post-mortem analysis was performed on tundish samples collected from two steel plants. One of the plants uses a DVM lining consisting primarily of periclase (~70 wt%) and olivine (~30 wt%) while the other employs an olivine-free DVM lining consisting primarily of periclase. The overall compositions of each are described in Table I. The casting conditions of each tundish are given in Table II. Both samples were taken from near the middle of each tundish, in a region that would have been in contact with both flux and steel as the fill level fluctuated between ladles. The samples were chiseled out of each tundish, cross sectioned, then mounted in epoxy for polishing.

Table I. Composition of the Tundish Linings

Tundish DVM	MgO	SiO_2	CaO	Al_2O_3	Fe_2O_3
Periclase/Olivine	82.9	11.8	1.5	1.1	2.3
Periclase Only	92.6	3.3	3.3	0.1	0.6

Table II. Casting Conditions of the Sampled Tundishes

Tundish DVM	Sequence Length	Steel Grades
Periclase/Olivine	6 heats	Low-C, Al-killed
Periclase Only	20 heats	Special Bar Quality

Laboratory Experiment

Samples for a laboratory experiment were formed by filling a 2”-diameter 4”-long pipe with approximately 250 g of DVM. The same DVMs used in the post-mortem analysis were used to create the samples. Steel pins were installed to aid in securing the samples in place during the experiment. A vibrating table was used to facilitate consolidation. The samples were then cured according to the typical protocol employed by each mill for their material.

The experiments were conducted in a 200 lbs. capacity coreless induction furnace. Two steel chemistries were used for the lab tests. Each tundish lining was paired with a steel that promotes congruence with the industrial post-mortems with the compositional details included as Table III (Future work will expose each lining to the same steel grade for a more thorough direct comparison.).

Table III. Chemistry of Steel Melted for each Experiment

		Steel Chemistry			
Tested Refractory	Sample RPM	C	Si	Mn	Cr
Periclase/Olivine	40	0.07	0.76	1.08	--
Periclase Only	30	0.29	0.24	0.63	0.45

Both steels in the present study were killed using Al shot. The steel paired with the high-periclase lining was also treated with Ca wire (Ca powder wrapped in a steel jacket). After each steel melt was prepared, the furnace power was adjusted to maintain 1550 °C. Upon reaching temperature, the refractory sample was introduced. To do so, the sample was suspended from a movable frame (illustrated in Figure 1) that was rolled over the furnace opening. The sample was then gradually lowered into the melt until the exposed end of the sample was submerged ~3/8” into the steel melt. To ensure the bottom surface of the refractory was only in contact with molten steel, vermiculite was used to help remove any slag that may have formed during the preparation of the steel melt. As an additional precaution, a low-carbon steel foil was used to cover the sample. Upon submersion of the sample, the motor controlling sample rotation was turned on (RPM listed in Table III). After 20 minutes, rotation was stopped, the sample

was removed, and the steel was cast into ingots to be discarded or used in future experiments. Upon cooling, each refractory sample was encased with epoxy before being sectioned then polished to 1 µm for microscopy.

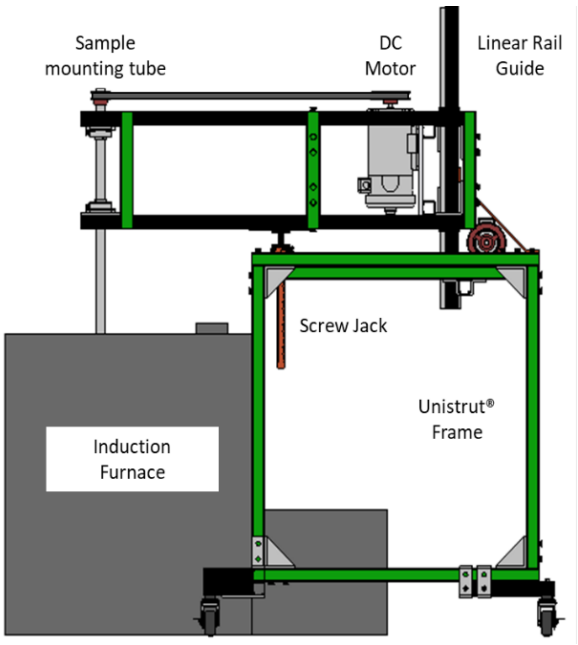

Figure 1. Schematic of the apparatus used for experiment.

For all samples, cathodoluminescence was employed using an optical microscope and camera with high-sensitivity/low-light capabilities. Cathodoluminescence (CL) is an optical technique that involves impinging a sample with a beam of electrons (10 kV) which for many refractory materials results in the emission of photons in the visible light spectrum. The color emitted is a function of the chemistry of the material and is influenced by trace elements and impurities. Therefore, CL is a useful technique for differentiating phases with greater clarity than typical optical microscopy at the same magnification. This leads to rapid identification of reaction layers and regions of interest for further analysis[6,7]. Scanning electron microscopy and energy dispersive spectroscopy was performed on regions of interest. Backscattered electron images were taken using an ASPEX Pica 1020 and a Tescan Vega-3. EDS measurements were taken using a Bruker X-Flash Silicon Drift Detector in the Tescan Vega-3.

RESULTS AND DISCUSSION

Post-Mortem

Figure 2 shows the periclase/olivine industrial post-mortem sample. Under CL, four main regions can be identified, here labeled A-D. The phases indicated in Figure 2 were determined through scanning electron microscopy and energy dispersive spectroscopy. An example of such an EDS measurement is shown in Figure 3. The first layer (Layer A) is a blue layer that appears to have been deposited on the surface on the refractory. This is mostly a calcium aluminate phase and is likely flux material that coated the surface of the lining upon draining. Behind the flux layer, an approximately 60 µm thick green layer (Layer B) is identified. This layer consists largely of magnesium aluminate spinel and delineates the surface of the refractory from the wetted flux material. Beyond Layer B is an approximately 3.5 mm thick region of dark purple crystallites that correspond to MgO (Layer C). Layers B and C are similar in color but differ in the size and quantity of crystallites. Layer C is depleted of the high SiO_2 phases found in the bulk of the refractory. This is the result of dissolution by the tundish cover flux, which would also explain why the Ca content of the matrix phase did not drop considering the original flux contained 42.5 wt% CaO. This is supported by other work by the authors of present paper, where silica depletion was found in periclase samples that were only in contact with flux[6]. As Layer C transitions into the bulk of the refractory, the MgO crystallites are shown to be grouped together into larger aggregates by monticellite (in yellow), appearing alongside dark grains

with orange borders (Layer D). These orange-bordered grains are olivine. The dark center is due to a higher concentration of iron. Iron and iron oxide do not respond to CL. This separation of phases occurred during the casting sequence

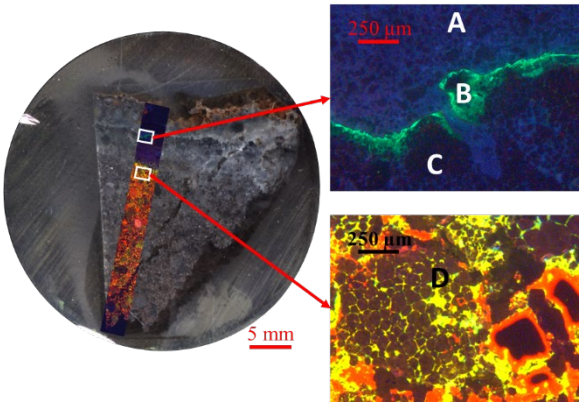

Figure 2. CL imagery of the periclase/olivine post-mortem sample.

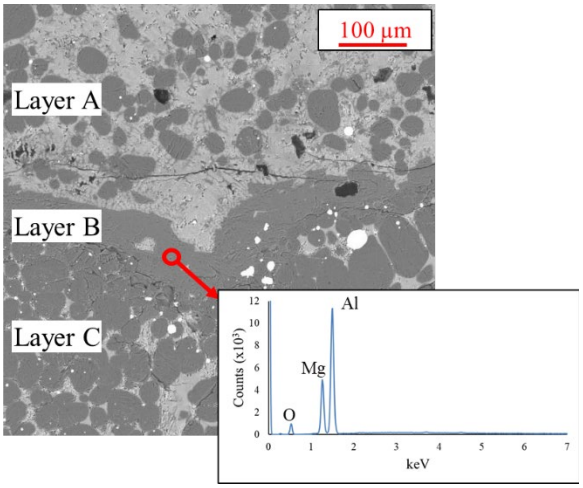

Figure 3. Example EDS measurement of Layer B in the periclase/olivine post-mortem sample.

Erosion of the refractory is also suggested by the presence of MgO particles in Layer A, remote to the surface of the refractory. The secondary phases interstitial to the MgO crystallites within the periclase aggregates have melting temperature below or close to that of steel. For example, monticellite melts at 1498 °C. It is possible, then, that periclase aggregates near the refractory/steel interface tend to lose or decline in mechanical integrity, and thereby compromise wear resistance.

Figure 4 shows the high-periclase industrial post-mortem sample. CL imagery illuminates three main regions. The green and red layer is deposited flux (Layer E), in which needle-like alumina crystallites have precipitated from a liquid calcium silicate-based phase as the tundish cooled after the casting sequence. Spinel is found primarily in Layer F. The bulk of the refractory (Layer G) shows seemingly unaffected periclase aggregates, though the secondary phases appear in bands of forsterite (Mg_2SiO_4, in red) and monticellite (in yellow green). Some of the forsterite phase does appear in the spinel region. However, no MgO crystallites are found in the spinel or flux layers, unlike the periclase/olivine industrial post-mortem where MgO was found on both sides of the spinel layer. The high-periclase tundish did experience a longer casting sequence, so it is possible that more of the MgO, eroded due to compromise of its binding phases, was able to react with Al_2O_3, which would result in the larger spinel layer.

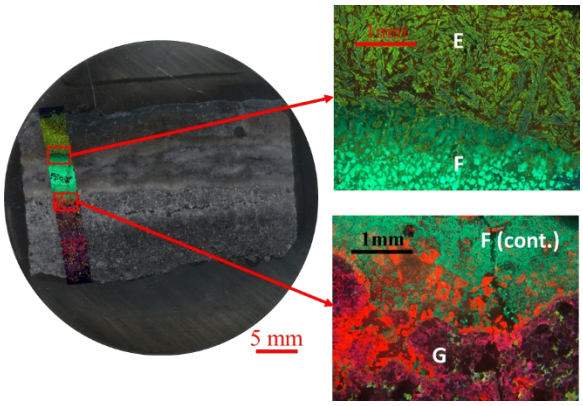

Figure 4. CL imagery of the periclase-only post-mortem sample.

Laboratory Experiment

Figure 5 shows a portion of the periclase/olivine laboratory sample. CL images across the sample indicate the presence of three main layers at the refractory/steel interface. At the surface of the refractory is a thin ~670 µm layer (Layer

A) showing similar colors as those seen in the bulk refractory, but with an altered morphology indicative of wear and interaction with the melt. This transitions to an approximately half millimeter thick layer of green (Layer B). The white stripe on the left side of the sample is an alumina pin of known pre-test length inserted into the sample, the "cold" end of which was to serve as a datum for post-mortem refractory wear quantification. Unfortunately, the pin shifted during vibration, so with this attempt, it cannot be relied on for measurement.

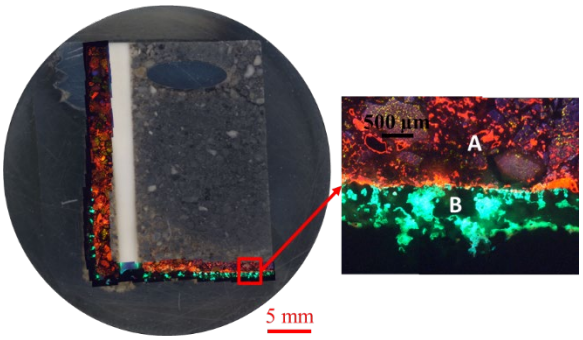

Figure 5. CL imagery of the periclase/olivine laboratory sample.

The phases were identified through x-ray diffraction (XRD). Before being mounted in epoxy and sectioned, a portion of Layer B was sampled from the surface, then ground and analyzed with XRD and presented as Figure 6. The four main phases identified were MgO, spinel, olivine, and corundum.

Figure 7 shows select EDS maps of the surface of the periclase/olivine laboratory refractory sample. Al is found throughout Layer B whereas Ca, Mg, and Si are found in higher concentrations in Layer A. An EDS survey of layer B further indicates that this layer consists of spinel (Figure 8). The remaining phases consist of various oxides that may have originated from either the worn refractory or reoxidized steel components. Literature[1,3,8] suggests multiple sources of oxygen for reoxidation of steel alloys. These sources include air trapped within porosity and easily reducible oxides. As an example, the iron oxide found in olivine may be a concern.

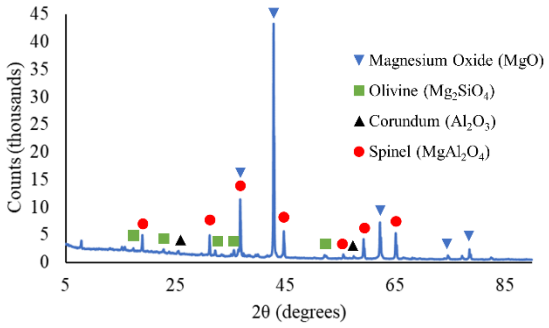

Figure 6. X-ray diffraction performed on the accretion formed on the periclase/olivine experimental sample.

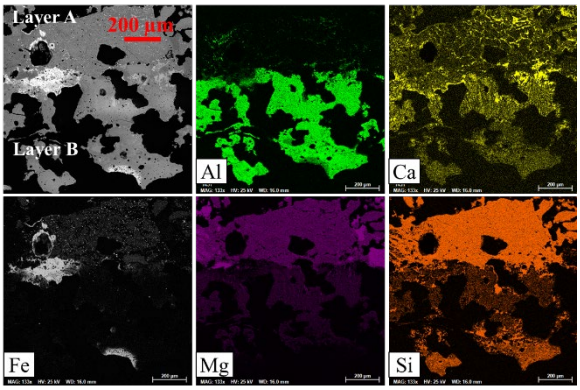

Figure 7. EDS Maps taken of Layers A and B of the periclase/olivine experimental sample.

The fact that the concentration of Ca and Si are both higher closer to the bulk of the refractory suggests that a portion of the Ca and Si found in these regions is likely to have originated in from the refractory, thereby indicating some erosion may have occurred resulting from the loss of the secondary intra-aggregate phase that binds the periclase crystallites. However, the high concentration of Fe and Si far from the bulk refractory also shows reoxidation was also possible. Iron oxide can further react with the MgO in the refractory forming magnesiowüstite ((Mg,Fe)O). However, this phase can also be formed by diffusion of iron oxide from the olivine aggregates to the periclase[9]. The Ca-rich phase indicated in

Figure 8 was not identified by XRD, which suggests either there is an insufficient amount of this phase to indicate, or this phase is amorphous in nature and does not present with peaks

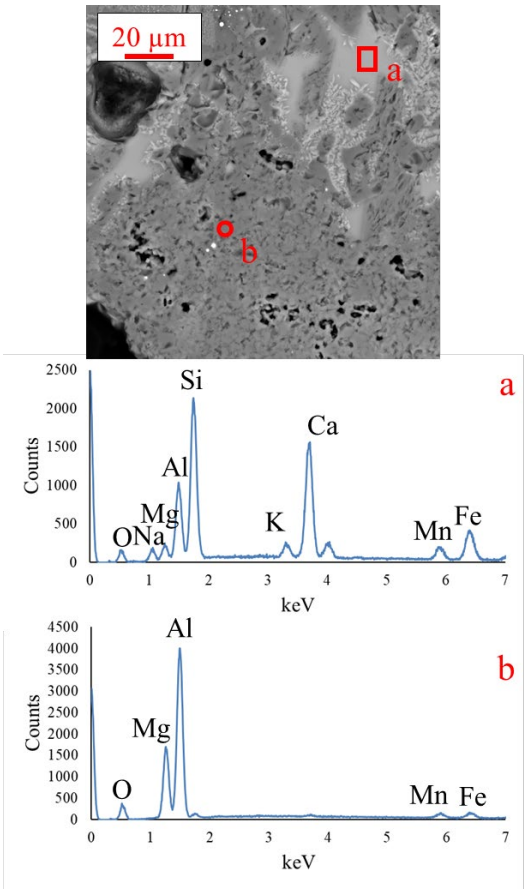

Figure 8. EDS measurements of the phases in Layer B.

Figure 9 shows a portion of the high-periclase laboratory sample. CL in this case presented only one distinct layer along the bottom melt-contact surface: an approximately 80-micron thick green layer (Layer C). However, there are clear signs of heavy infiltration and erosion at the melt line, further indicated by the presence of a predominately red phase in the CL imagery. Backscattered electron microscopy of Layer C indicates multiple phases are present (Figure 10). Similar to the periclase/olivine laboratory sample, a magnesium aluminate spinel phase is predominate. Unlike the periclase/olivine sample, it is less clear from EDS whether any of the Ca and Si originated from the refractory. In fact, a notable amount of calcium aluminate is found on the outer portion of this layer. It is possible, then, that this is the agglomeration of calcium aluminate inclusions due to the calcium addition to the steel in this experiment. Overall, the changes in morphology that signaled refractory wear in the periclase/olivine laboratory sample are not readily apparent in the high-periclase sample. This could explain why the periclase/olivine laboratory sample exhibited a thicker, open structure for its spinel layer when compared to the thinner, condensed spinel layer in the high periclase laboratory sample. The presence of spinel suggests that, either way, some of the refractory must have been consumed in the reaction. This somewhat mimics the comparison between the industrial post-mortem samples, though in the case of the high-periclase example, some forsterite possibly originating from the refractory was found in the spinel layer, whereas the laboratory experimental sample showed a distinct delineation between layers.

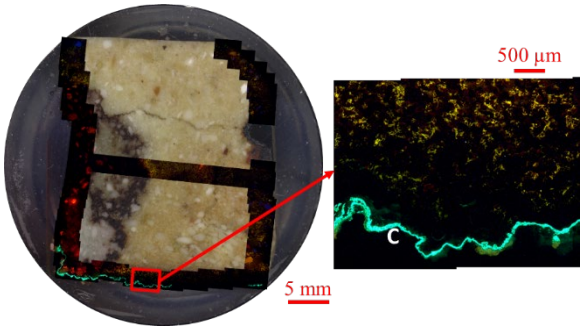

Figure 9. CL imagery of the periclase-only experimental sample.

EDS indicated approximately 20 wt% Mn throughout the heavily infiltrated region on the left side of the sample. The Mn could only have originated from the steel as this is foreign to the refractory composition. The fact that only the side is affected suggests that this corrosion was by an unintended slag layer that developed during the experiment.

The consequences of this slag formation on the other observed phenomena will need exploration with future experiments. However, as the bottom of the refractory was protected from any inadvertent slag contact during insertion by the steel foil and was otherwise only in contact with steel while submerged, it is unlikely that this slag would have directly interacted with the refractory in the regions analyzed in Figure 10.

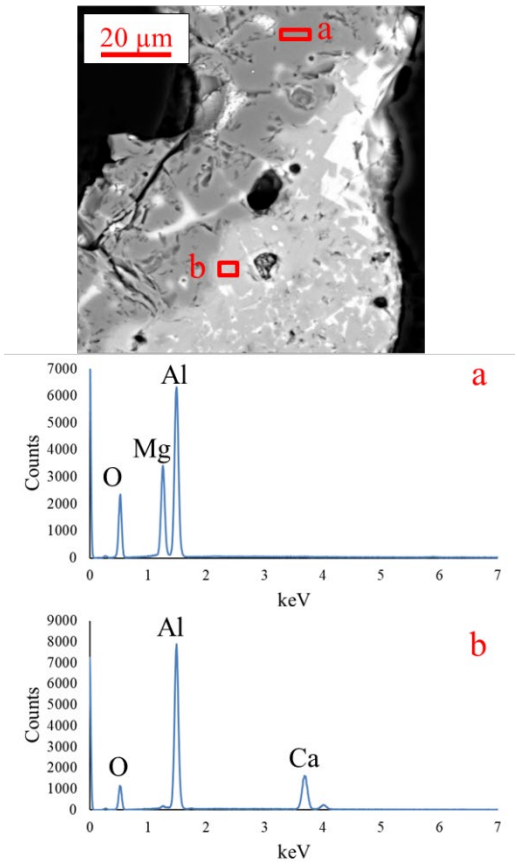

Figure 10. EDS measurements of Layer C. The dark grey phase is spinel and the light gray phase is calcium aluminate. The brightest phase is a Ca-rich aluminosilicate.

Spinel formation is a concern of the steel industry as spinel inclusions are solid at steelmaking temperature and take on an angular morphology that is detrimental to the mechanical properties of the final product. Multiple reaction models have been suggested for how spinel might form in a steelmaking environment. One is the direct reaction between MgO, Al, and O as described by Reaction (1) and (2)[4] :

$$3MgO_{(s)} + 2\underline{Al} = 3\underline{Mg} + Al_2O_{3\,(s)} \quad (1)$$

$$\underline{Mg} + Al_2O_{3(s)} + \underline{O} = MgAl_2O_{4\,(s)} \quad (2)$$

Other models involve the reduction of MgO by C, Al, or Si. The product of this reduction is either Mg dissolved in the steel or a Mg vapor that reoxidizes in the steel melt, then reacts with Al or Al_2O_3 to form spinel[5]. An example of Al reduction was observed in tundish linings with significant SiO_2 content by Mantovani *et al.*[1], where Si was substituted by Al in the magnesium silicate phase. This reaction can be described by Reaction (3).

$$3\,Mg_2SiO_{4\,(s)} + 4[Al] = 2\,MgAl_2O_{4\,(s)} + 4\,MgO_{(s)} + 3[Si] \quad (3)$$

Determining which mechanism(s) is responsible for the generation of spinel requires an understanding of the activities of the possible reactants and how they relate to the amount of products generated, as well as the kinetics of the reactions in the tundish. Given how easily the periclase aggregates can be removed from the lining (at least, in the case of the periclase/olivine lining), the direct reaction model appears plausible. As the periclase/olivine post-mortem sample displayed a depletion of Si in regions infiltrated by alumina-rich flux, it would seem Reaction (3) may also be possible. However, this phenomenon was not replicated in the lab test, as the depletion of silica in the refractory is a result of interaction with flux, not steel.

When comparing the two industrial post-mortem samples, certain parameters should be acknowledged. The two tundishes sampled experienced casting sequences of differing lengths and steel grades. The periclase/olivine tundish was used to cast six ladles of low-carbon steel with Ti additions,

whereas the high-periclase tundish was used to cast 20 heats of low-alloy special bar quality steel. While the minor constituents of either steel grade were not detected in the post-mortem EDS analysis, their impacts on the observed phenomena may need further exploration. Similar parameters should be acknowledged when comparing the industrial post-mortems to the lab test samples. While spinel was able to form without flux (in fact, direct interactions with flux did not result in the formation of a spinel layer in previous work[6]), it is possible that interactions with cover flux may impact the mobility of MgO for the reaction (note the presence of MgO crystallites suspended in the flux layer in Figure 2). It is also possible that morphology and size of the spinel layer is affected by exposure duration.

CONCLUSIONS

Post-mortem analysis has been performed on two DVM linings, one consisting of a mixture of periclase and olivine and the other containing no olivine. Although spinel formation was noted in both samples, the morphology and thickness differed. Additionally, the bulk of the refractory was significantly impacted in the periclase/olivine lining, in that Si depletion was significant in areas infiltrated by flux. A laboratory experiment was performed and showed that refractory erosion and spinel formation can occur due to interactions with the steel, regardless of the presence of flux.

REFERENCES

1. M. C. Mantovani, L. R. Moraes Jr, R. Leandro da Silva, E. F. Cabral, E. A. Possente, C. A. Barbosa, and B. P. Ramos, "Interactions between molten steel and different kinds of MgO based tundish linings." *Ironmaking & Steelmaking*, 40 [5] 319-325 (2013)

2. M. Kalantar, B. M. Moshtaghioun, and A. Monshi, "Developing Two New Tundish Plasters and Comparing with the Magnesia Plaster Used in Continuous Casting of Steel." *Journal of Materials Engineering and Performance* 19 [2] 237-245 (2010)

3. A. Pack, S. Hoernes, T. Walther, and R. Bross, "Behavior of basic refractories at high temperatures in steelmaking processes – thermodynamic and implications for the usability of olivine as refractory material." *European Journal of Mineralogy*, 15 [1] 193-205 (2003)

4. H. Itoh, M. Hino, and S. Ban-ya, "Thermodynamics on the formation of spinel nonmetallic inclusions in liquid steel." *Metallurgical and Materials Transactions B*, 28 [5] 953-956 (1997)

5. G. Okuyama, K. Yamaguchi, S. Takeuchi, and K.I. Sorimachi, "Effect of slag composition on the kinetics of formation of Al2O3-MgO inclusions in aluminum killed ferritic stainless steel." *ISIJ International*, 40 [2] 121-128 (2000)

6. T.M. Richards, R.J. O'Malley, J.D. Smith, and T.P. Sander, "Interactions between Molten Tundish Slags and Periclase/Periclase-Olivine Tundish Linings." *ACerS Refractory Ceramics Division Symposium on Refractories*, St. Louis, Missouri, March 2021

7. M. Karakus and R. Moore, "Cathodoluminescence (CL) Microscopy Application to Refractories and Slags." *Journal of Minerals and Materials Characterization and Engineering* 1 [1] 11-29 (2002)

8. Y. Liu, G. Li, L. Wang, and Z. Zhang, "Effect of the Tundish Gunning Materials on the Steel Cleanliness." *High Temperature Materials and Processes*, 37 [4] 313-323 (2018)

9. A.R. Pal, S. Bharati, S. Bose, S.K. Choudhury, G.C. Das, and P.G. Pal, "Effect of component variation in CaO-SiO_2-MgO-Al_2O_3 slags on controlling corrosion of olivine based disposable tundish lining

material." *Ironmaking and Steelmaking*, 40 [7] 515-520 (2013)